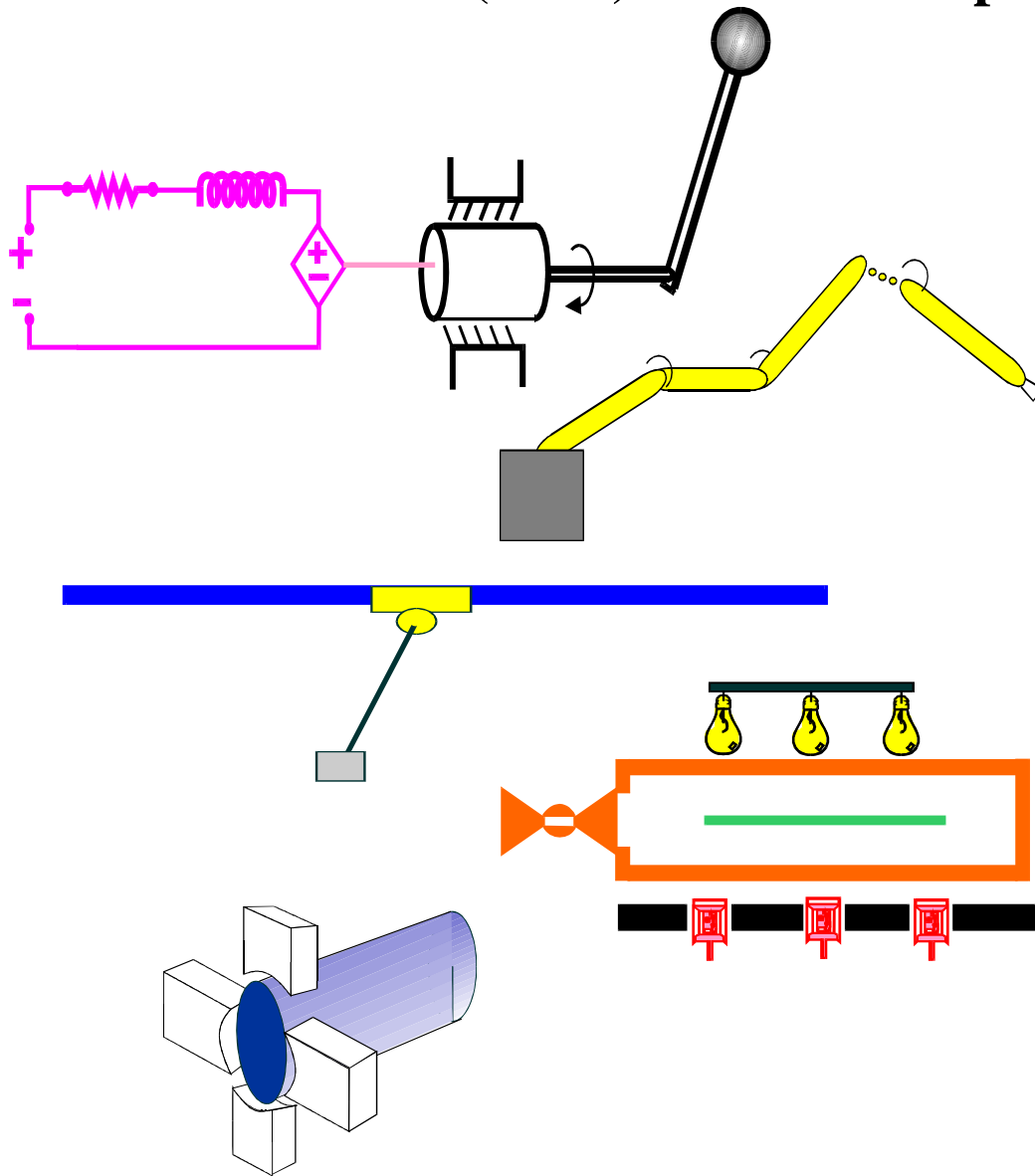


**Clemson University**  
**College of Engineering and Science**  
**Control and Robotics (CRB) Technical Report**



Number: CU/CRB/8/30/05/#1

Title: Adaptive Nonlinear Tracking Control  
of Kinematically Redundant Robot  
Manipulators with Sub-Task Extensions

Authors: E. Tatlicioglu, M. McIntyre, D. Dawson,  
and I. Walker

# Adaptive Nonlinear Tracking Control of Kinematically Redundant Robot Manipulators with Sub-Task Extensions<sup>1</sup>

E. Tatlicioglu, M. McIntyre, D. Dawson, and I. Walker

Department of Electrical & Computer Engineering, Clemson University, Clemson, SC 29634-0915

E-mail: mmcinty@ces.clemson.edu

**Abstract:** Past research efforts have focused on the end-effector tracking control of redundant robots because of their increased dexterity over their non-redundant counterparts. This work utilizes an adaptive full-state feedback quaternion based controller developed in [5] and focuses on the design of a general sub-task controller. This sub-task controller does not affect the position and orientation tracking control objectives, but instead projects a preference on the configuration of the manipulator based on sub-task objectives such as the following: singularity avoidance, joint limit avoidance, bounding the impact forces, and bounding the potential energy.

## 1 Introduction

In many robotic applications, the desired task is naturally defined in terms of end-effector motion. As a result, the desired robot trajectory is described by the desired position and orientation of a Cartesian coordinate frame attached to the robot manipulator's end-effector with respect to the base frame, also referred to as the *task-space*. Control of robot motion is then performed using feedback of either the joint variables (relative position of each robot joint pair) or the task-space variables. Unfortunately, joint-based control has the undesirable feature of requiring the solution of the inverse kinematics to convert the desired task-space trajectory into the desired joint space trajectory. In contrast, task-space control does not require the inverse kinematics; however, the precise tracking control of the end-effector orientation complicates the problem. For example, several parameterizations exist to describe the orientation angles, including minimum three-parameter representations (*e.g.*, Euler angles, Rodrigues parameters, *etc.*) and the non-minimum four-parameter representation given by the unit quaternion. Whereas the three-parameter representations always exhibit singular orientations (*i.e.*, the orientation Jacobian matrix in the kinematic equation is singular for some orientations), the unit quaternion-based approach can be used to represent the end-effector orientation without singularities. Thus, despite significantly complicating

the control design, the unit quaternion seems to be the preferred method of formulating the end-effector orientation tracking control problem. Some past work that deals with task-space control formulation can be found in [2], [9], and [22]. Specifically, an experimental assessment of different end-effector orientation parameterization for task-space robot control was provided in [2]. One of the first results in task-space control of robot manipulators was presented in [9]. Resolved-rate and resolved-acceleration task-space controllers using the quaternion parameterization were proposed in [22].

In addition, the control problem is further complicated in the presence of kinematic redundancy. That is, to provide the end user with increased flexibility for executing sophisticated tasks, the next generation of robot manipulators will have more degrees of freedom than are required to perform an operation in the task-space. Since the number of joints in a redundant robot is greater than the dimension of the task-space, one can show that joint motion in the null-space of the Jacobian matrix exists that does not affect task-space motion (this phenomenon is commonly referred to as *self-motion*). As noted in [14], [15], and [19], there are generally an infinite number of solutions for the inverse kinematics of redundant robots. As a result, given a desired task-space trajectory, it is difficult to select a reasonable desired joint trajectory that satisfies the control requirements (*e.g.*, closed-loop stability and boundedness of all signals) and the sub-tasks (*e.g.*, singularity avoidance, joint limit avoidance, bounding the impact forces and bounding the potential energy). Thus, there is strong motivation for control of redundant robots to be done in the task-space. For work related to controllers for redundant robots, the reader is referred to [3], [6], [9], [16], [18], [21], [23] and the references therein.

This paper utilizes the adaptive full-state feedback quaternion based controller developed in [5] and focuses on the design of a general sub-task controller. The novelty of this work is the systematic integration of the sub-task controller while simultaneously achieving end-effector tracking. Other efforts have been proposed in [5], [6] and [23], but in these approaches, the sub-task objective is an *add-on* to the tracking objec-

---

<sup>1</sup>This research was supported in part by two DOC Grants, an ARO Automotive Center Grant, a DOE Contract, a Honda Corporation Grant, and a DARPA Contract.

tive without integration into the stability analysis. In [5], a sub-task control signal was introduced and can be seen in equation (2.211) as  $h(t)$ . In the stability analysis of [5], this sub-task signal is inconsequential to the tracking control objective as long as  $h(t)$  and  $\dot{h}(t)$  remain bounded. This work will exploit the property of self-motion for redundant robot manipulators by designing a general sub-task controller that meets the above conditions while controlling the joint motion in the null-space of the Jacobian matrix to alleviate potential problems in the physical system or select configurations that are better suited for a particular application. Specific sub-task controllers will be designed for singularity avoidance, joint limit avoidance, bounding the impact forces and bounding the potential energy. In Section 2 the dynamic and kinematic models are described for a general redundant robot manipulator. In Section 3 the tracking objective is presented. The tracking closed-loop error system is presented in Section 4. In Sections 5 and 6, both the general sub-task controller as well as four specific sub-task controllers are presented. A numerical simulation was completed for each specific sub-task and the results are presented in Section 7. Concluding remarks are made in Section 8.

## 2 Robot Dynamic and Kinematic Model

The dynamic model for an  $n$ -joint ( $n \geq 6$ ), revolute, direct drive robot manipulator is described by the following expression

$$M(\theta)\ddot{\theta} + V_m(\theta, \dot{\theta})\dot{\theta} + G(\theta) + F_d\dot{\theta} = \tau \quad (1)$$

where  $\theta(t), \dot{\theta}(t), \ddot{\theta}(t) \in \mathbb{R}^n$  denote the joint position, velocity, and acceleration in the joint-space, respectively. In (1),  $M(\theta) \in \mathbb{R}^{n \times n}$  represents the inertia effects,  $V_m(\theta, \dot{\theta}) \in \mathbb{R}^{n \times n}$  represents centripetal-Coriolis effects,  $G(\theta) \in \mathbb{R}^n$  represents the gravity effects,  $F_d \in \mathbb{R}^{n \times n}$  represents the constant positive definite diagonal dynamic frictional effects,  $\tau(t) \in \mathbb{R}^n$  represents the control input torque vector. The subsequent development is based on the following properties [12].

**Property 1:** The inertia matrix  $M(\theta)$  is symmetric and positive-definite, and satisfies the following inequalities

$$m_1 \|\xi\|^2 \leq \xi^T M(\theta)\xi \leq m_2 \|\xi\|^2 \quad \forall \xi \in \mathbb{R}^n \quad (2)$$

where  $m_1, m_2 \in \mathbb{R}$  are positive constants, and  $\|\cdot\|$  denotes the standard Euclidean norm.

**Property 2:** The inertia and centripetal-Coriolis matrices satisfy the following skew symmetric relationship

$$\xi^T \left( \frac{1}{2} \dot{M}(\theta, \dot{\theta}) - V_m(\theta, \dot{\theta}) \right) \xi = 0 \quad \forall \xi \in \mathbb{R}^n \quad (3)$$

where  $\dot{M}(\theta, \dot{\theta})$  denotes the time derivative of the inertia matrix.

**Property 3:** The left-hand side of (1) can be linearly parameterized as shown below

$$M(\theta)\ddot{\theta} + V_m(\theta, \dot{\theta})\dot{\theta} + G(\theta) + F_d\dot{\theta} = Y_g(\theta, \dot{\theta}, \ddot{\theta})\phi \quad (4)$$

where  $\phi \in \mathbb{R}^p$  contains the constant system parameters, and the regression matrix  $Y_g(\cdot) \in \mathbb{R}^{n \times p}$  contains known functions dependent on the signals  $\theta(t), \dot{\theta}(t)$ , and  $\ddot{\theta}(t)$ .

Let  $\mathcal{E}$  and  $\mathcal{B}$  be orthogonal coordinate frames attached to the end-effector of a redundant robot manipulator and its inertial frame, respectively. The position and orientation of  $\mathcal{E}$  relative to  $\mathcal{B}$  are commonly represented by a homogeneous transformation matrix,  $T(\theta) \in \mathbb{R}^{4 \times 4}$  which is defined as [12]

$$T(\theta) \triangleq \begin{bmatrix} R(\theta) & p(\theta) \\ 0_{1 \times 3} & 1 \end{bmatrix} \quad (5)$$

where  $0_{1 \times 3} \triangleq [0 \ 0 \ 0]$ , the vector  $p(\theta) \in \mathbb{R}^3$  and the rotation matrix  $R(\theta) \in \mathbb{R}^{3 \times 3}$  represent the position and orientation of the end-effector coordinate frame, respectively. From this homogeneous transformation matrix, the constrained four-parameter unit quaternion representation can be used to develop the kinematic model. From (5), a relationship between the position and orientation of  $\mathcal{E}$  relative to  $\mathcal{B}$  can be developed as follows [13]

$$\begin{bmatrix} p \\ q \end{bmatrix} \triangleq \begin{bmatrix} f_p(\theta) \\ f_q(\theta) \end{bmatrix} \quad (6)$$

where  $f_p(\theta) \in \mathbb{R}^3$  and  $f_q(\theta) \in \mathbb{R}^4$  are kinematic functions,  $q(t) \triangleq [q_o(t) \ q_v^T(t)]^T \in \mathbb{R}^4$  with  $q_o(t) \in \mathbb{R}$  and  $q_v(t) \in \mathbb{R}^3$ . The variable  $q(t)$ , as given in (6), denotes the unit quaternion [7]. The unit quaternion represents a *global nonsingular* parameterization of the end-effector orientation, and is subject to the constraint  $q^T q = 1$ . Note that, while  $f_p(\theta)$  is directly obtained from (5), several algorithms exist to determine  $f_q(\theta)$  from  $R(\theta)$  ([7] and [10]). Conversely,  $R(q)$  can be determined given the unit quaternion parameterization [7]

$$R(q) \triangleq (q_o^2 - q_v^T q_v) I_3 + 2q_v q_v^T + 2q_o q_v^\times \quad (7)$$

where  $I_3 \in \mathbb{R}^{3 \times 3}$  is the standard identity matrix, and the notation  $a^\times \in \mathbb{R}^{3 \times 3} \forall a = [a_1 \ a_2 \ a_3]^T$ , denotes the following skew-symmetric matrix

$$a^\times \triangleq \begin{bmatrix} 0 & -a_3 & a_2 \\ a_3 & 0 & -a_1 \\ -a_2 & a_1 & 0 \end{bmatrix}. \quad (8)$$

Velocity relationships can be formulated by differentiating (6) which can be written as

$$\begin{bmatrix} \dot{p} \\ \dot{q} \end{bmatrix} = \begin{bmatrix} J_p(\theta) \\ J_q(\theta) \end{bmatrix} \dot{\theta} \quad (9)$$

where  $\dot{\theta}(t) \in \mathbb{R}^n$  denotes the velocity of  $\mathcal{E}$  in a generalized coordinate system, and  $J_p(\theta) \in \mathbb{R}^{3 \times n}$ ,  $J_q(\theta) \in \mathbb{R}^{4 \times n}$  denotes the position and orientation Jacobian matrices, respectively. To facilitate the subsequent control development and stability analysis, the fact that  $q(t)$  is related to the angular velocity of  $\mathcal{E}$  relative to  $\mathcal{B}$ , denoted by  $\omega(t) \in \mathbb{R}^3$  with coordinates expressed in  $\mathcal{B}$ , via the following differential equation ([1] and [13])

$$\dot{q} \triangleq B(q)\omega \quad (10)$$

where the Jacobian-type matrix  $B(q) \in \mathbb{R}^{4 \times 3}$  is defined as follows

$$B(q) \triangleq \frac{1}{2} \begin{bmatrix} -q_v^T \\ q_o I_3 - q_v^\times \end{bmatrix} \quad (11)$$

where  $B(q)$  satisfies the following useful property

$$B^T(q)B(q) = I_3. \quad (12)$$

The final kinematic expression that relates the generalized Cartesian velocity to the generalized coordinate system is developed as follows

$$\begin{bmatrix} \dot{p} \\ \omega \end{bmatrix} = J(\theta) \dot{\theta} \quad (13)$$

where (9), (10) and (12) were utilized, and  $J(\theta) \in \mathbb{R}^{6 \times n}$  is defined as follows

$$J(\theta) \triangleq \begin{bmatrix} J_p(\theta) \\ B^T(q)J_q(\theta) \end{bmatrix}. \quad (14)$$

To facilitate the control development, the pseudo-inverse of  $J(\theta)$  is denoted by  $J^+(\theta) \in \mathbb{R}^{n \times 6}$ , which is defined as follows

$$J^+ \triangleq J^T (JJ^T)^{-1} \quad (15)$$

where  $J^+(\theta)$  satisfies the following equality

$$JJ^+ = I_6 \quad (16)$$

where  $I_6 \in \mathbb{R}^{6 \times 6}$  is the standard identity matrix. As shown in [14], the pseudo-inverse defined by (15) satisfies the Moore-Penrose Conditions given below

$$\begin{aligned} JJ^+J &= J & J^+JJ^+ &= J^+ \\ (J^+J)^T &= J^+J & (JJ^+)^T &= JJ^+. \end{aligned} \quad (17)$$

In addition to the above properties, the matrix  $(I_n - J^+J)$  satisfies the following useful properties

$$\begin{aligned} (I_n - J^+J)(I_n - J^+J) &= I_n - J^+J \\ (I_n - J^+J)^T &= (I_n - J^+J) \\ J(I_n - J^+J) &= 0 \\ (I_n - J^+J)J^+ &= 0 \end{aligned} \quad (18)$$

where  $I_n \in \mathbb{R}^{n \times n}$  is the standard identity matrix.

**Remark 1** During the control development, the assumption that the minimum singular value of the manipulator Jacobian, denoted by  $\sigma_m$  is greater than a known small positive constant  $\delta > 0$ , such that  $\max \{\|J^+(\theta)\|\}$  is known a priori and all kinematic singularities are always avoided.

**Remark 2** The dynamic and kinematic terms for a general revolute robot manipulator, denoted by  $M(\theta)$ ,  $V_m(\theta, \dot{\theta})$ ,  $G(\theta)$ ,  $J(\theta)$ , and  $J^+(\theta)$ , are assumed to depend on  $\theta(t)$  only as arguments of trigonometric functions, and hence, remain bounded for all possible  $\theta(t)$ . During the control development, the assumption will be made that if  $p(t) \in \mathcal{L}_\infty$  then  $\theta(t) \in \mathcal{L}_\infty$  (Note that  $q(t)$  is always bounded since  $q(t)^T q(t) = 1$ ).

### 3 Task-Space Tracking

The objective for the redundant robotic system is to design a control input that ensures the position and orientation of  $\mathcal{E}$  tracks the position and orientation of a desired orthogonal coordinate frame  $\mathcal{E}_d$  where  $p_d(t) \in \mathbb{R}^3$  denotes the position of the origin of  $\mathcal{E}_d$ , relative to the origin of  $\mathcal{B}$  and the rotation matrix from  $\mathcal{E}_d$  to  $\mathcal{B}$  is denoted by  $R_d(\cdot) \in \mathbb{R}^{3 \times 3}$ . The standard assumption that  $p_d(t)$ ,  $\dot{p}_d(t)$ ,  $\ddot{p}_d(t)$ ,  $R_d(\cdot)$ ,  $\dot{R}_d(\cdot)$ , and  $\ddot{R}_d(\cdot) \in \mathcal{L}_\infty$  will be utilized in the subsequent stability analysis. The position tracking error  $e_p(t) \in \mathbb{R}^3$  can be defined as follows

$$e_p \triangleq p_d - p \quad (19)$$

where  $p(t)$  was defined in (5). If the orientation of  $\mathcal{E}_d$  relative to  $\mathcal{B}$  is described by the desired unit quaternion,  $q_d(t) \triangleq [q_{od}(t) \ q_{vd}^T(t)]^T \in \mathbb{R}^4$ , then similar to (7), the desired rotation matrix can be described as follows

$$R_d(q_d) = (q_{od}^2 - q_{vd}^T q_{vd}) I_3 + 2q_{vd} q_{vd}^T + 2q_{od} q_{vd}^\times. \quad (20)$$

As in (10),  $q_d(t)$  is related to the desired angular velocity of  $\mathcal{E}_d$  relative to  $\mathcal{B}$ , denoted by  $\omega_d(t) \in \mathbb{R}^3$ , through the kinematic equation

$$\dot{q}_d \triangleq B(q_d)\omega_d. \quad (21)$$

To quantify the difference between the actual and desired end-effector orientations, a rotation matrix  $\tilde{R}(\cdot) \in \mathbb{R}^{3 \times 3}$  of  $\mathcal{E}$  with respect to  $\mathcal{E}_d$  is defined as follows

$$\tilde{R} \triangleq R_d^T R = (e_o^2 - e_v^T e_v) I_3 + 2e_v e_v^T + 2e_o e_v^\times \quad (22)$$

where the unit quaternion tracking error,  $e_q(t) \triangleq [e_o(t) \ e_v^T(t)]^T \in \mathbb{R}^4$  can be derived as follows (see [22] and Theorem 5.3 of [11])

$$e_q \triangleq \begin{bmatrix} e_o \\ e_v \end{bmatrix} = \begin{bmatrix} q_o q_{od} + q_v^T q_{vd} \\ q_{od} q_v - q_o q_{vd} + q_v^\times q_{vd} \end{bmatrix} \quad (23)$$

where  $e_q(t)$  satisfies the constraint

$$e_q^T e_q = e_0^2 + e_v^T e_v = 1, \quad (24)$$

which indicates that

$$0 \leq \|e_v(t)\| \leq 1 \quad 0 \leq |e_0(t)| \leq 1 \quad (25)$$

for all time.

Based on the above definitions, the end-effector position and orientation tracking objectives can be stated as follows

$$\|e_p(t)\| \rightarrow 0 \text{ and } \tilde{R}(e_q) \rightarrow I_3 \text{ as } t \rightarrow \infty, \quad (26)$$

respectively. The orientation tracking objective given in (26) can also be stated in terms of the unit quaternion error of (23). Specifically, it is easy to see from (24) that

$$\text{if } \|e_v(t)\| \rightarrow 0 \text{ as } t \rightarrow \infty, \text{ then } |e_0(t)| \rightarrow 1 \text{ as } t \rightarrow \infty; \quad (27)$$

hence, it can be stated from (22) and (27) that

$$\text{if } \|e_v(t)\| \rightarrow 0 \text{ as } t \rightarrow \infty, \text{ then } \tilde{R}(e_q) \rightarrow I_3 \text{ as } t \rightarrow \infty. \quad (28)$$

#### 4 Task-Space Controller

Based on the open-loop kinematic tracking error system given in [5] and the subsequent stability analysis, the control input is designed as follows

$$\tau \triangleq Y\hat{\phi} + K_r r + (\Lambda J)^T \begin{bmatrix} e_p \\ e_v \end{bmatrix} \quad (29)$$

where  $K_r \in \mathbb{R}^{n \times n}$  is a positive-definite, diagonal, control gain matrix, and  $\hat{\phi}(t) \in \mathbb{R}^p$  denotes the parameter estimate vector which is updated according to

$$\dot{\hat{\phi}} \triangleq \Gamma Y^T r \quad (30)$$

with  $\Gamma \in \mathbb{R}^{p \times p}$  being a positive-definite, diagonal, adaptation gain matrix. The auxiliary signal  $r(t) \in \mathbb{R}^n$  can be defined as follows

$$r \triangleq u_d - \dot{\theta} \quad (31)$$

where  $u_d(t) \in \mathbb{R}^n$  is an auxiliary control input defined as follows

$$u_d \triangleq J^+ \Lambda^{-1} \begin{bmatrix} \dot{p}_d + K_1 e_p \\ -R_d^T \omega_d + K_2 e_v \end{bmatrix} + (I_n - J^+ J) h \quad (32)$$

where  $K_1, K_2 \in \mathbb{R}^{3 \times 3}$  are positive-definite, diagonal, control gain matrices, the matrix  $\Lambda(t) \in \mathbb{R}^{6 \times 6}$  is defined as follows

$$\Lambda \triangleq \begin{bmatrix} -I_3 & 0_{3 \times 3} \\ 0_{3 \times 3} & R_d^T \end{bmatrix} \quad (33)$$

where  $0_{3 \times 3} \in \mathbb{R}^{3 \times 3}$  denotes a matrix of zeros, and  $h(\theta) \in \mathbb{R}^n$  is the subsequently designed sub-task controller signal. The linear parameterization  $Y(p_d, \dot{p}_d, \ddot{p}_d, e_q, \theta, \dot{\theta}, h, \dot{h})\phi$  introduced in (29) is defined as follows

$$Y\phi \triangleq M\dot{u}_d + V_m u_d + G(\theta) + F_d \dot{\theta} \quad (34)$$

where  $Y(\cdot) \in \mathbb{R}^{n \times p}$  denotes the measurable regression matrix, and  $\phi \in \mathbb{R}^p$  represents the constant parameter vector (e.g., mass, inertia, and friction coefficients). To obtain the closed-loop dynamics for  $r(t)$ , the time derivative of (31) is taken, pre-multiply the resulting equation by  $M(\theta)$ , and substitute (1) to obtain the following

$$M\dot{r} = -V_m r + Y\tilde{\phi} - K_r r - (\Lambda J)^T \begin{bmatrix} e_p \\ e_v \end{bmatrix} \quad (35)$$

where the parameter estimation error signal  $\tilde{\phi}(t) \in \mathbb{R}^p$  is defined as follows

$$\tilde{\phi} \triangleq \phi - \hat{\phi}. \quad (36)$$

**Remark 3** A benchmark adaptive controller was utilized to compensate for the parametric uncertainties present in the dynamic model (e.g., mass, inertia, and friction coefficients). Alternatively, a robust or sliding mode controller could also be used to compensate for modeling uncertainties not restricted to parametric uncertainties (e.g. see [4]).

The following theorem can be stated regarding the stability of the closed loop system.

**Theorem 1** The control law described by (29) guarantees global asymptotic end-effector position and orientation tracking in the sense that

$$\|e_p(t)\| \rightarrow 0 \text{ as } t \rightarrow \infty \quad (37)$$

and

$$\tilde{R}(e_q(t)) \rightarrow I_3 \text{ as } t \rightarrow \infty, \quad (38)$$

as well as that all signals are bounded provided  $h(\theta) \in \mathcal{L}_\infty$  and  $\frac{\partial h(\theta)}{\partial \theta} \in \mathcal{L}_\infty$ . (Note the assumption given in Remark 2 has been utilized.)

**Proof:** See [5] for proof.

#### 5 Sub-Task Control Objective

In addition to the tracking control objective, there can be sub-task objectives that are required for a particular redundant robot application. To this end, the auxiliary control signal  $h(\theta)$ , as introduced in (32), allows for sub-task objectives to be integrated into the controller. This sub-task integration is completed by designing a

framework that places preferences on desirable configurations where an infinite number of choices are available when dealing with the *self-motion* of the redundant robot. These sub-tasks are integrated through the joint motion in the null-space of the standard Jacobian matrix by designing  $h(\theta)$ . Theorem 1 requires that  $h(\theta)$ ,  $\frac{\partial h(\theta)}{\partial \theta} \in \mathcal{L}_\infty$ , provided  $\theta(t) \in \mathcal{L}_\infty$ . Based on Remark 2, and the proof of Theorem 1 it is clear that  $\theta(t) \in \mathcal{L}_\infty$ . In the subsequent section,  $h(\theta)$  will be designed to meet these conditions. In the event that a subsequently defined Jacobian-related matrix loses rank, the sub-task objective is not guaranteed. More specifically, if the Jacobian-related matrix maintains full rank, then the sub-task objective is met as proven in the subsequent stability analysis.

## 6 Sub-Task Closed-Loop Error System

In this section, a general sub-task closed-loop error system is developed. To this end, an auxiliary signal  $y_a(t) \in \mathbb{R}^+$  is defined as follows

$$y_a \triangleq \exp(-\alpha\beta(\theta)) \quad (39)$$

where  $\alpha \in \mathbb{R}^+$  is a constant,  $\beta(\theta) \in \mathbb{R}^+$  is selected for each sub-task, and  $\exp(\cdot)$  is the standard logarithmic exponential function. To determine the dynamics of  $y_a(t)$ , the time derivative of (39) is taken and can be written as follows

$$\dot{y}_a = J_s \dot{\theta} \quad (40)$$

where a Jacobian-type vector  $J_s(t) \in \mathbb{R}^{1 \times n}$  is defined as follows

$$J_s = \frac{\partial y_a}{\partial \theta}. \quad (41)$$

From (40), a substitution can be made for  $\dot{\theta}(t)$  and the following expression for  $\dot{y}_a(t)$  can be written as follows

$$\begin{aligned} \dot{y}_a &= J_s J^+ \Lambda^{-1} \begin{bmatrix} \dot{p}_d + K_1 e_p \\ -R_d^T \omega_d + K_2 e_v \end{bmatrix} \\ &+ J_s (I_n - J^+ J) h - J_s r \end{aligned} \quad (42)$$

where (31) and (32) were both utilized. Based on the dynamics of (42) and the subsequent stability analysis, the sub-task control input can be designed as follows

$$h \triangleq -k_{s1} [J_s (I_n - J^+ J)]^T y_a \quad (43)$$

where  $k_{s1} \in \mathbb{R}^+$  is a constant gain. After substituting (43) into (42), the following expression can be obtained

$$\begin{aligned} \dot{y}_a &= J_s J^+ \Lambda^{-1} \begin{bmatrix} \dot{p}_d + K_1 e_p \\ -R_d^T \omega_d + K_2 e_v \end{bmatrix} \\ &- J_s r - k_{s1} \|J_s (I_n - J^+ J)\|^2 y_a. \end{aligned} \quad (44)$$

**Remark 4** The auxiliary signal  $y_a(t)$  in (39) was selected because of the useful properties of the logarithmic exponential function. From (39) it is clear that

$0 < y_a(t) \leq 1$ , and that as  $\beta(\theta)$  increases,  $y_a(t)$  decreases. This definition of  $y_a(t)$  is arbitrary and many different positive functions could also be utilized.

The following theorem can now be stated regarding the performance of the sub-task closed-loop error system.

**Theorem 2** The control law described by (43) guarantees that  $y_a(t)$  is practically regulated (i.e., ultimately bounded) in the following sense

$$|y_a(t)| \leq \sqrt{|y_a^2(t_0)| \exp(-2\gamma t) + \frac{\varepsilon}{\gamma}} \quad (45)$$

provided the following sufficient conditions hold

$$\|J_s (I_n - J^+ J)\|^2 > \bar{\delta} \quad (46)$$

and

$$k_{s1} > \frac{1}{\delta \delta_2} \quad (47)$$

where  $\varepsilon, \gamma, \bar{\delta}, \delta_2 \in \mathbb{R}^+$  are constants.

**Proof:** See Appendix A.

**Remark 5** In the subsequent sub-sections, specific  $\beta(\theta)$  functions will be designed for different sub-task objectives. Each  $\beta(\theta)$  is designed specifically to only depend on  $\theta(t)$ . For most of the sub-task objectives, the problem is set up to require that  $\beta(\theta) > 0$  which is achieved by keeping  $y_a(t) < 1$ . From (45), it is clear that  $y_a(t) < 1$  if the following inequality holds

$$\sqrt{|y_a^2(t_0)| + \frac{\varepsilon}{\gamma}} < 1 \quad (48)$$

which can be achieved through the selection of the robot manipulator's initial condition, control gains  $k_{s1}$ ,  $\alpha$ , and bounding constants. For other sub-task objectives, the problem is to maximize  $\beta(\theta)$  as  $t \rightarrow \infty$  (minimize  $y_a(t)$  as  $t \rightarrow \infty$ ). From the result of Theorem 2 as seen in (45), a true maximization of  $\beta(\theta)$  (minimization of  $y_a(t)$ ) is not achieved. However, an increasing lower bound for  $\beta(\theta)$  (an exponentially decreasing upper bound for  $y_a(t)$ ) is achieved from (45).

**Remark 6** The four sub-task objectives as described in the subsequent sub-sections are met only if the sufficient conditions as described by (46) and (47) are met. These sub-task objectives are secondary to the tracking objective which is always guaranteed by Theorem 1. In the event that the sub-task controller attempts to force the robot manipulator's end-effector to take a path not allowed by the tracking controller, the condition in (46) will not be met; hence, the result of Theorem 2 will not hold. With this fact in mind, the formulation of the desired task-space trajectory and the sub-task objectives require careful consideration to meet both the tracking and sub-task objectives simultaneously.

### 6.1 Sub-Task 1: Singularity Avoidance

The objective for this sub-task is to keep the robot manipulator away from configurations that result in singularities, and hence, decrease the manipulability of the robot manipulator. For this sub-task, let  $\beta(\theta)$  be defined as the manipulability measure of a robot manipulator given by the following definition [17]

$$\beta = \sqrt{\det [JJ^T]} \quad (49)$$

where  $\det[\cdot]$  is the determinant of the  $6 \times 6$  matrix  $J(\theta)J^T(\theta)$  and  $\beta(\theta) = 0$  when the robot is in a singular configuration. From (39), (45), (48), and (49), it is clear that  $\beta(\theta) > 0 \forall t$ , provided the sufficient conditions are met, hence meeting this sub-task objective.

### 6.2 Sub-Task 2: Joint Limits

Joint limits are a mechanical constraint for almost all robot manipulators. In (1), the joint angles represented by  $\theta_i(t) \in \mathbb{R}^+ \forall i = 1..n$  operate in the range of  $\theta_i \in [\theta_i^{\min} \theta_i^{\max}]$ , where  $\theta_i^{\min}, \theta_i^{\max} \in \mathbb{R}^+$  are the minimum and maximum joint limits for each joint, respectively. The objective for this sub-task is to keep each joint angle away from its respective joint limits, while executing the tracking control objective. For this sub-task, the auxiliary signal  $\beta(\theta)$  is defined as follows

$$\beta \triangleq \prod_{i=1}^n \left[ \left( 1 - \frac{\theta_i}{\theta_i^{\max}} \right) \left( \frac{\theta_i}{\theta_i^{\min}} - 1 \right) \right]. \quad (50)$$

From (50), it is clear that  $\beta(\theta) > 0$  as long as all joints are not at the joint limits. From (39), (45), (48), and (50), it is clear that  $\beta(\theta) > 0 \forall t$ , provided the sufficient conditions are met, hence meeting this sub-task objective.

### 6.3 Sub-Task 3: Impact Force Configurations

For collision applications of robotic manipulators, the user often requires the ability to specify the impact force the end-effector makes with the environment. For hammering, or chiseling applications, the user may want to maximize the impact force, while in a medical application, the desire to have reduced collision force may be necessary. To study these concepts, an impact force measure is defined as,  $F(t) \in \mathbb{R}$ , which can be written as follows [20]

$$F \triangleq \frac{-(1 + \kappa) \vartheta^T \eta}{\eta^T J M^{-1} J^T \eta} \quad (51)$$

where  $\kappa \in \mathbb{R}$  denotes the type of collision ( $\kappa$  is either zero or one),  $\vartheta(t) \in \mathbb{R}^3$  is the velocity vector for the two colliding bodies, and  $\eta(t) \in \mathbb{R}^3$  is a vector normal to the plane of contact for the two colliding bodies,  $M(\theta) \in \mathbb{R}^{n \times n}$  is the inertia matrix as found in (1). Utilizing (51), impact force sub-task objectives can be defined to either upper or lower bound the impact force with the environment.

### 6.3.1 Upper Bounding the Impact Force:

The objective for this sub-task is to keep the robot manipulator away from postures that are “best” suited for impact with the environment for a given end-effector velocity and point of contact, hence  $\vartheta(t)$  and  $\eta(t)$  are predetermined and fixed. To this end,  $\beta(\theta)$ , is defined as the denominator of (51), and can be written as follows [20]

$$\beta = \eta^T J M^{-1} J^T \eta. \quad (52)$$

Large values of  $\beta(\theta)$  indicate postures with small impact forces at the end-effector [20]; therefore, the goal of this sub-task is to force the manipulator into postures that results in larger values of  $\beta(\theta)$ . From (39), (45), (48), and (52), it is clear that  $\beta(\theta(t)) > 0 \forall t$ , provided the sufficient conditions are met.

### 6.3.2 Withstanding Impacts:

An alternate impact sub-task is to push the robot manipulator into postures that are “best” suited to withstand impacts with the environment. For this case, let  $\beta(\theta)$  be defined as the *dynamic impact measure* given by the following definition [20]

$$\beta \triangleq \sqrt{\det [(J^+)^T M^2 J^+]}. \quad (53)$$

Large values of  $\beta(\theta)$  indicate postures with high impact forces at the end-effector [20]; therefore, the goal of this sub-task is to force the manipulator into postures that results in larger values of  $\beta(\theta)$ . From (39), (45), (48), and (53), it is clear that  $\beta(\theta(t)) > 0 \forall t$ , provided the sufficient conditions are met.

**Remark 7** For the adaptive control paradigm, the constant parameters for the inertia matrix  $M(\theta)$  are not precisely known; therefore, estimates of these parameters must be utilized in (52) and (53) in lieu of the actual values. The matrix inverse of the estimate of  $M(\theta)$  (i.e.,  $\hat{M}(\theta)$ ) can be guaranteed through the use of a projection as described in [8].

### 6.4 Sub-Task 4: Upper Bounding the Potential Energy

The objective for this sub-task is to keep the robot manipulator away from postures that result in an unnecessarily high level of potential energy. With the flexibility inherent to redundant robots, a posture with less potential energy is more desirable, thus providing an increase in system efficiency. The potential energy,  $\mu(t) \in \mathbb{R}$ , stored in the manipulator can be defined as follows [17]

$$\mu \triangleq - \sum_{i=1}^n [m_{li} g_o^T P_{li} + m_{mi} g_o^T P_{mi}] \quad (54)$$

where  $m_{li}, m_{mi} \forall i = 1..n$  are the joint and rotor masses, respectively,  $g_o \triangleq [0 \ 0 \ -g]^T$ , is the gravitational acceleration vector in the base frame where  $g$

is the gravitational constant,  $P_{mi}(\theta) \in \mathbb{R}^3$  is a vector from the origin of the base frame  $\mathcal{B}$  to the center position of the rotor, and  $P_{li}(\theta) \in \mathbb{R}^3$  is a vector described as follows [17]

$$P_{li} \triangleq \frac{1}{m_{li}} \int_{V_{li}} P_i^* \rho dV \quad (55)$$

where  $\rho \in \mathbb{R}$  is the density of the elementary particle of volume  $dV$ ,  $P_i^*(\theta) \in \mathbb{R}^3$  is a vector from the origin of  $\mathcal{B}$  to the center joint position. From (54) and (55), it is clear that  $\mu(t)$  is a function of  $\theta(t)$  and by convention is always positive. For this sub-task, the auxiliary signal  $y_a(t) \in \mathbb{R}$  is defined as follows

$$y_a \triangleq \mu(\theta). \quad (56)$$

The goal is to force the manipulator to take postures with less potential energy. From (45), (48), and (56), provided the sufficient conditions are met, it is clear that by making the control gain  $k_{s1}$  large,  $\gamma$  is made large (See Appendix A), and by examining (45), it is clear that the potential energy will have an exponentially decreasing upper bounded.

**Remark 8** *For the adaptive control paradigm, the constant parameters for the rotor and joint masses are not precisely known; therefore, estimates of these parameters must be utilized in (54) and (55) in lieu of the actual values as discussed in Remark 7.*

## 7 Simulation Results

To illustrate the performance of the tracking and sub-task controller presented above, a simplified kinematic simulation was completed for a planar 3-joint revolute robot. This robot is redundant because there are 3 joints in a 2 dimensional task-space. For the simulation, a feedback linearization controller was utilized, and hence the adaptation mechanism was not required<sup>1</sup>. Specifically, the following dynamic model was utilized

$$M(\theta) \ddot{\theta} + N(\theta, \dot{\theta}) = \tau \quad (57)$$

where  $\ddot{\theta}(t)$ ,  $\tau(t) \in \mathbb{R}^3$ , the inertia matrix  $M(\theta) \in \mathbb{R}^{3 \times 3}$  is defined as follows

$$M(\theta) = \begin{bmatrix} M_{11} & M_{12} & M_{13} \\ M_{12} & M_{22} & M_{23} \\ M_{13} & M_{23} & M_{33} \end{bmatrix}$$

where

$$\begin{aligned} M_{11} &= p_1 + 2p_4c_2 + 2p_5c_2c_3 + 2p_6c_3 & M_{22} &= p_2 + 2p_6c_3 \\ M_{12} &= p_2 + p_4c_2 + p_5c_2c_3 + 2p_6c_3 & M_{23} &= p_2 + p_6c_3 \\ M_{13} &= p_2 + p_5c_2c_3 + p_6c_3 & M_{33} &= p_3 \end{aligned}$$

<sup>1</sup>A feedback linearization controller was utilized, as opposed to an adaptive controller, to more clearly illustrate the performance of the sub-task objective.

where  $p_1 = 1.2746$  [kg·m<sup>2</sup>],  $p_2 = 0.3946$  [kg·m<sup>2</sup>],  $p_3 = 0.0512$  [kg·m<sup>2</sup>],  $p_4 = 0.4752$  [kg·m<sup>2</sup>],  $p_5 = 0.128$  [kg·m<sup>2</sup>],  $p_6 = 0.1152$  [kg·m<sup>2</sup>] and  $c_2 \triangleq \cos(\theta_2)$ ,  $c_3 \triangleq \cos(\theta_3)$ , and  $c_{23} \triangleq \cos(\theta_2 + \theta_3)$ ,  $N(\theta, \dot{\theta}) \in \mathbb{R}^3$  represents the centripetal-Coriolis, gravitational and frictional effects. For the potential energy simulations given below, the gravitational effects  $G(\theta) = [G_1(\theta) \ G_2(\theta) \ G_3(\theta)]^T$  where  $G_1(\theta), G_2(\theta), G_3(\theta) \in \mathbb{R}$  are defined as follows

$$\begin{aligned} G_1(\theta) &= \frac{1}{2}m_{l1}gl_1c_1 + m_{l2}g(l_1c_1 + \frac{1}{2}l_2c_1c_2) \\ &\quad + m_{l3}g(l_1c_1 + l_2c_1c_2 + \frac{1}{2}l_3c_1c_2c_3) \end{aligned}$$

$$G_2(\theta) = \frac{1}{2}m_{l2}gl_2c_1c_2 + m_{l3}g(l_2c_1c_2 + \frac{1}{2}l_3c_1c_2c_3)$$

$$G_3(\theta) = \frac{1}{2}m_{l3}gl_3c_1c_2c_3$$

where the center of mass is at the midpoint of each joint, and was selected as follows:  $m_{l1} = 3.6$  [kg],  $m_{l2} = 2.6$  [kg], and  $m_{l3} = 2$  [kg], the joint lengths were selected as follows:  $l_1 = 0.40$  [m],  $l_2 = 0.36$  [m], and  $l_3 = 0.32$  [m], the gravitational constant was selected as follows:  $g = 9.8$  [ $\frac{m}{sec^2}$ ], and  $c_1 \triangleq \cos(\theta_1)$ ,  $c_{12} \triangleq \cos(\theta_1 + \theta_2)$ ,  $c_{123} \triangleq \cos(\theta_1 + \theta_2 + \theta_3)$ ,  $s_1 \triangleq \sin(\theta_1)$ ,  $s_{12} \triangleq \sin(\theta_1 + \theta_2)$ , and  $s_{123} \triangleq \sin(\theta_1 + \theta_2 + \theta_3)$ . Feedback linearization can be used to linearize (57) as follows

$$M(\theta) U_c + N(\theta, \dot{\theta}) = \tau \quad (58)$$

where  $U_c(t) \in \mathbb{R}^3$  is the inner loop control input. After substituting (58) into (57), we have

$$\ddot{\theta} = U_c. \quad (59)$$

The task-space is defined by  $x(t) \in \mathbb{R}^2$ , where  $x(t) \triangleq [x_1(t) \ x_2(t)]^T$ , and  $x_1(t), x_2(t) \in \mathbb{R}$  are scalar euclidean coordinates. The planar 3-joint robot has the following forward kinematics for the end-effector

$$\begin{bmatrix} x_1 \\ x_2 \end{bmatrix} \triangleq \begin{bmatrix} l_1c_1 + l_2c_1c_2 + l_3c_1c_2c_3 \\ l_1s_1 + l_2s_1c_2 + l_3s_1c_2c_3 \end{bmatrix} \quad (60)$$

and the manipulator Jacobian

$$\begin{aligned} J(q) &\triangleq \begin{bmatrix} -l_1s_1 - l_2s_1c_2 - l_3s_1c_2c_3 & & \\ l_1c_1 + l_2c_1c_2 + l_3c_1c_2c_3 & & \\ -l_2s_1c_2 - l_3s_1c_2c_3 & -l_3s_1c_2c_3 & \\ l_2c_1c_2 + l_3c_1c_2c_3 & l_3c_1c_2c_3 & \end{bmatrix} \end{aligned} \quad (61)$$

The elimination of the dynamics and rotational tracking requirement simplifies the control problem, therefore it is necessary to redefine some key terms to establish a simplified closed-loop error system. The position

tracking error signal  $e(t) \in \mathbb{R}^2$  can now be defined as follows

$$e \triangleq x_d - x \quad (62)$$

where the desired trajectory  $x_d(t) \in \mathbb{R}^2$  is generated by the following bounded dynamic system

$$\begin{bmatrix} \dot{x}_{d1} \\ \dot{x}_{d2} \end{bmatrix} \triangleq \begin{bmatrix} -0.05 \sin(0.1t) \\ 0.004 (\cos(0.1t))^2 - 0.004 (\sin(0.1t))^2 \end{bmatrix} \quad (63)$$

and can be seen in Figure 1. The auxiliary control input

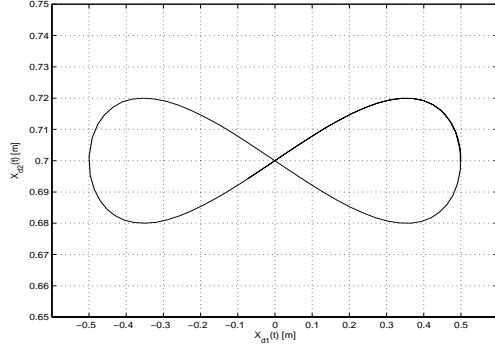


**Figure 1:** Desired trajectory for three link robot.

$u_d(t)$  as defined in (32) can be simplified as follows

$$u_d \triangleq J^+ (K_s e + \dot{x}_d) + (I_3 - J^+ J) h \in \mathbb{R}^3 \quad (64)$$

where  $K_s \in \mathbb{R}^{2 \times 2}$  is a positive-definite, diagonal, control gain matrix. The inner loop control input is defined as follows

$$U_c \triangleq k_o r + \dot{u}_d + J^T e \quad (65)$$

where  $k_o \in \mathbb{R}^+$  is a positive control gain. The simplified closed-loop error system can now be written as follows

$$\dot{r} = -k_o r - J^T e. \quad (66)$$

To demonstrate the performance of all the sub-task controllers, a different simulation was completed for each sub-task. The initial conditions for the robot manipulator in each sub-task were intentionally selected to make  $\beta(\theta(t_0)) \approx 0$  (i.e. maximize  $y_a(t_0)$ ) to demonstrate that (45) holds for each simulation run. In the case of the potential energy sub-task, the initial conditions for the robot manipulator was selected to maximize  $\mu(t_0)$ .

### 7.1 Singularity Avoidance

To demonstrate the sub-task controller's performance for singularity avoidance as described by (39), (43) and (49), the robot manipulator was initially at rest at the following joint positions (i.e.  $\beta(\theta(t_0)) \approx 0$ ):

$$\theta(t_0) = [0.45[\text{rad}] \quad 0.0[\text{rad}] \quad 3.1[\text{rad}]]^T$$

with the gains selected as follows

$$K_s = \text{diag}\{2, 2\}, \quad k_0 = 2, \quad k_{s1} = 1 \quad \text{and} \quad \alpha = 4$$

where  $\text{diag}\{\cdot\}$  denotes a diagonal matrix with arguments along the diagonal. Both the tracking and singularity avoidance sub-task were successfully demonstrated, and can be seen by the following figures: the manipulability measure  $\beta(\theta)$  and the tracking error can be seen in Figures 2 and 3, respectively.

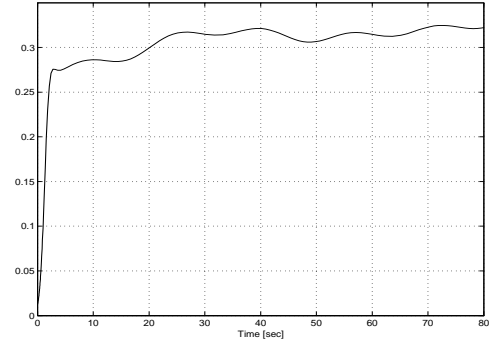


**Figure 2:** Manipulability Measure

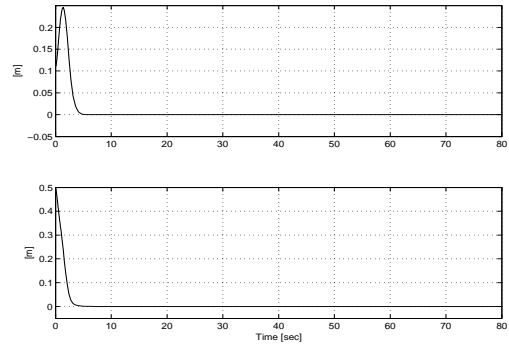


**Figure 3:** Tracking Error

### 7.2 Joint Limits

To demonstrate the sub-task controller's performance for joint limit avoidance as described by (39), (43), and (50), the robot manipulator was initially at rest at the following joint positions (i.e.  $\beta(\theta(t_0)) = 0$ ):

$$\theta(t_0) = [0.5[\text{rad}] \quad 1.5[\text{rad}] \quad 3.5[\text{rad}]]^T$$

with the gains selected as follows

$$K_s = \text{diag}\{1, 4\}, \quad k_0 = 8, \quad k_{s1} = 1 \quad \text{and} \quad \alpha = 1.$$

The joint limits were set to the following values

$$\begin{aligned} \theta_1^{\min} &= \theta_2^{\min} = 0.5[\text{rad}] \quad \text{and} \quad \theta_3^{\min} = 0.1[\text{rad}] \\ \theta_1^{\max} &= \theta_2^{\max} = 2[\text{rad}] \quad \text{and} \quad \theta_3^{\max} = 6[\text{rad}]. \end{aligned}$$

Both the tracking and joint limits sub-task were successfully demonstrated and can be seen by the following figures: the auxiliary signal  $\beta(\theta)$  and the tracking error can be seen in Figures 4 and 5, respectively.

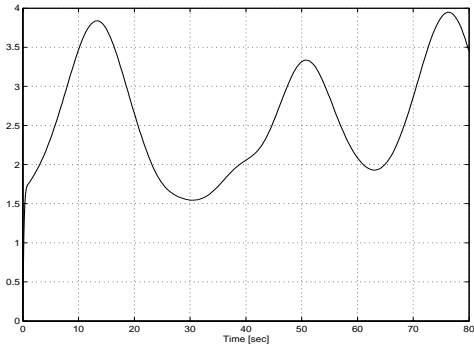


**Figure 4:**  $\beta(\theta)$  for Joint Limits Sub-Task

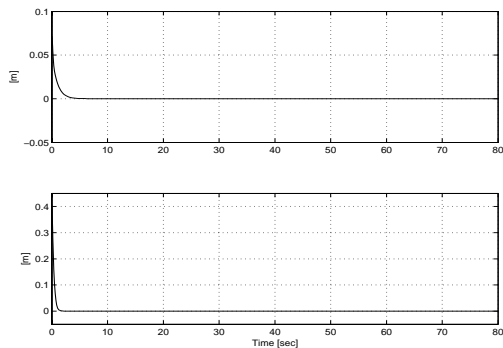


**Figure 5:** Tracking Error

### 7.3 Impact Force Configurations

#### 7.3.1 Upper Bounding the Impact Force:

To demonstrate the sub-task controller's performance for upper bounding the impact force as described by (39), (43) and (52), the robot manipulator was initially at rest at the following joint positions:

$$\theta(t_0) = [ 0.45[\text{rad}] \quad 0.0[\text{rad}] \quad 2.9[\text{rad}] ]^T \quad (67)$$

with the gains selected as follows

$$K_s = \text{diag}\{4, 4\}, k_0 = 3, k_{s1} = 1 \text{ and } \alpha = 8.$$

The initial conditions as described in (67) places the robot in a configuration resulting in  $\beta(\theta(t_0)) \approx 0$ , (i.e. a configuration with a high impact force potential). For this simulation, a plane of contact that is always perpendicular to  $x_1$  axis is assumed, so  $\eta(t) = [ 1 \quad 0 ]^T$

and is fixed. Although contact is never made, the sub-task controller works to place the robot in a configuration with less impact force potential (i.e.  $\beta(\theta(t)) > \beta(\theta(t_0))$ ). Both the tracking and upper bounding the impact force sub-task were successfully demonstrated and can be seen by the following figures: the denominator of (51) which was defined as  $\beta(\theta)$  and the tracking error can be seen in Figures 6 and 7, respectively.

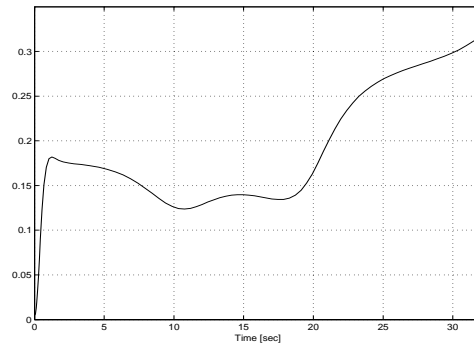


**Figure 6:**  $\beta(\theta)$  for Upper Bounding the Impact Force Sub-Task

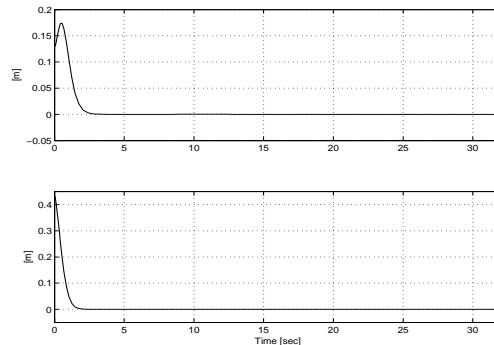


**Figure 7:** Tracking Error

#### 7.3.2 Withstanding Impacts:

To demonstrate the sub-task controller's performance for withstanding impacts as described by (39), (43) and (53), the robot manipulator was initially at rest at the following joint positions:

$$\theta(t_0) = [ 0.1[\text{rad}] \quad 1.7[\text{rad}] \quad 4.5[\text{rad}] ]^T \quad (68)$$

with the gains selected as follows

$$K_s = \text{diag}\{1, 1\}, k_0 = 4, k_{s1} = 1 \text{ and } \alpha = 1.$$

The initial conditions as described in (68) places the robot in a configuration with a high impact force potential. For this simulation, a plane of contact that is

always perpendicular to desired trajectory is assumed. Although contact is never made, the sub-task controller works to place the robot in a configuration with greater impact force potential (i.e.  $\beta(\theta(t)) > \beta(\theta(t_0))$ ). Both the tracking and withstanding impacts sub-task were successfully demonstrated and can be seen by the following figures: the withstanding impacts measure  $\beta(\theta)$  and the tracking error can be seen in Figures 8 and 9, respectively.

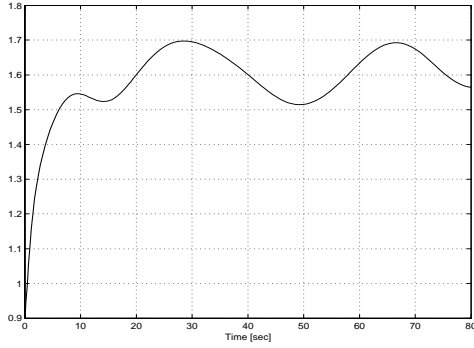


**Figure 8:**  $\beta(\theta)$  for Withstanding Impacts Sub-Task

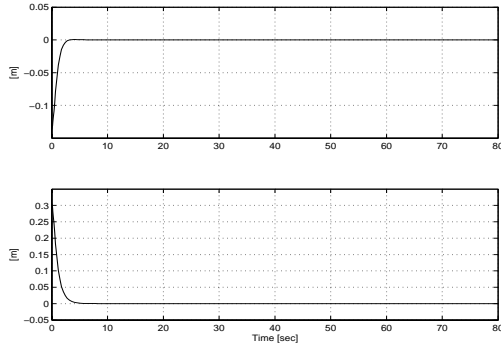


**Figure 9:** Tracking Error

#### 7.4 Upper Bounding the Potential Energy

To demonstrate the sub-task controller’s performance for upper bounding the potential energy as described by (43) and (56), the robot manipulator was initially at rest at the following joint positions:

$$\theta(t_0) = [ 1.57[rad] \quad 0.1[rad] \quad 0.48[rad] ]^T$$

with the gains selected as follows

$$K_s = \text{diag}\{1, 1\}, \quad k_0 = 2 \text{ and } k_{s1} = 1.$$

Both the tracking and upper bounding the potential energy sub-task were successfully demonstrated and can

be seen by the following figures: the potential energy measure  $\mu(\theta)$  and the tracking error can be seen in Figures 10 and 11, respectively.

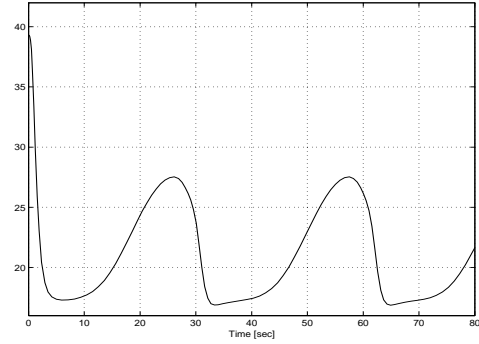


**Figure 10:**  $\mu(\theta)$  for Upper Bounding the Potential Energy Sub-Task

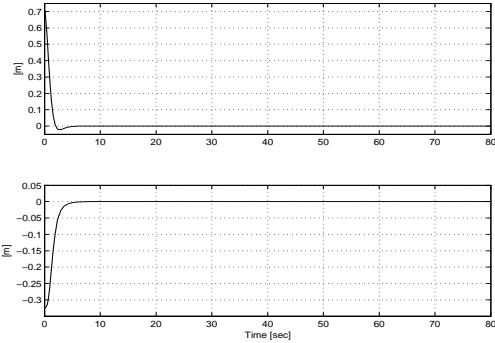


**Figure 11:** Tracking Error

## 8 Conclusions

This work utilized an adaptive full-state feedback quaternion based controller developed in [5] and focused on the design of a general sub-task controller. This general sub-task controller was developed as to not affect the tracking control objective, and allows for the design of specific sub-task objectives. Four specific sub-tasks were designed as follows: singularity avoidance, joint-limit avoidance, bounding the impact forces, and bounding the potential energy. Simulation results are presented that demonstrates both the tracking and sub-task objectives were met simultaneously.

## References

- [1] J. Ahmed, V. T. Coppola, and D. S. Bernstein, “Adaptive Asymptotic Tracking of Spacecraft Attitude Motion with Inertia Matrix Identification”, *J. Guidance, Control, and Dynamics*, Vol. 21, No. 5, pp. 684-691 (1998).

[2] F. Caccavale, C. Natale, B. Siciliano, and L. Villani, "Resolved-Acceleration Control of Robot Manipulators: A Critical Review with Experiments", *Robotica*, Vol. 16, No. 5, pp. 565-573, (1998).

[3] R. Colbaugh and K. Glass, "Robust Adaptive Control of Redundant Manipulators", *J. Intelligent and Robotic Systems*, Vol. 14, No. 1, pp. 68-88, (1995).

[4] D. M. Dawson, M. M. Bridges, and Z. Qu, "Nonlinear Control of Robotic Systems for Environmental Waste and Restoration", Englewood Cliffs, NJ: Prentice-Hall, 1995.

[5] W. E. Dixon, A. Behal, D. M. Dawson, and S. Nagarkatti, *Nonlinear Control of Engineering Systems: A Lyapunov-Based Approach*, Boston, MA: Birkhäuser, 2003.

[6] P. Hsu, J. Hauser, and S. Sastry, "Dynamic Control of Redundant Manipulators", *J. of Robotic Systems*, Vol. 6, No. 3, pp. 133-148, (1989).

[7] P. C. Hughes, *Spacecraft Attitude Dynamics*, New York, NY: Wiley, 1994.

[8] H. K. Khalil, "Adaptive Output Feedback Control of Nonlinear Systems Represented by Input-Output Models", *IEEE Trans. Automatic Control*, Vol. 41, No. 2, pp. 177-188, (1996).

[9] O. Khatib, "Dynamic Control of Manipulators in Operational Space", *IFTOMM Cong. Theory of Machines and Mechanisms*, December, New Delhi, India, 1983, pp. 1-10.

[10] A. R. Klumpp, "Singularity-Free Extraction of a Quaternion from a Directional Cosine Matrix", *J. Spacecraft and Rockets*, Vol. 13, No. 12, pp. 754-755, (1976).

[11] J. B. Kuipers, *Quaternions and Rotation Sequences*, Princeton, NJ: Princeton University Press, 1999.

[12] F. L. Lewis, D. M. Dawson, and C. T. Abdallah, *Robot Manipulator Control: Theory and Practice*, New York, NY: Marcel Dekker, Inc., 2004.

[13] F. Lizarralde and J. T. Wen, "Attitude Control Without Angular Velocity Measurement: A Passivity Approach", *IEEE Trans. Automatic Control*, Vol. 41, No. 3, pp. 468-472, (1996).

[14] Y. Nakamura, "Advanced Robotics Redundancy and Optimization", Reading, MA: Addison-Wesley, 1991.

[15] D. N. Nenchev, "Redundancy Resolution through Local Optimization: A Review", *J. Robotic Systems*, Vol. 6, No. 6, pp. 769-798, (1989).

[16] Z. X. Peng and N. Adachi, "Compliant Motion Control of Kinematically Redundant Manipulators", *IEEE Trans. Robotics and Automation*, Vol. 9, No. 6, pp. 831-837, (1993).

[17] L. Sciavicco and B. Siciliano, *Modeling and Control of Robot Manipulators*, New York, NY: McGraw-Hill Co., 1996.

[18] H. Seraji, "Configuration Control of Redundant Manipulators: Theory and Implementation", *IEEE Trans. Robotics and Automation*, Vol. 5, No. 4, pp. 472-490, (1989).

[19] B. Siciliano, "Kinematic Control of Redundant Robot Manipulators: A Tutorial", *J. Intelligent and Robotic Systems*, Vol. 3, pp. 201-212, (1990).

[20] I. D. Walker, "Impact Configurations and Measures for Kinematically Redundant and Multiple Armed Robot Systems," *IEEE Trans. on Robotics and Automation*, Vol. 10, No. 5, pp. 670-683 (1994).

[21] T. Yoshikawa, "Analysis and Control of Robot Manipulators with Redundancy", *Robotics Research - The First International Symp.*, Cambridge, MA, 1984, pp. 735-747.

[22] J. S. C. Yuan, "Closed-Loop Manipulator Control Using Quaternion Feedback", *IEEE Trans. Robotics and Automation*, Vol. 4, No. 4, pp. 434-440, (1988).

[23] E. Zergeroglu, D. M. Dawson, I. Walker, and A. Behal, "Nonlinear Tracking Control of Kinematically Redundant Robot Manipulators", *Proc. American Control Conf.*, June 28-30, Chicago, IL, 2000, pp. 2513-2517.

## Appendix

### A Proof of Theorem 2

Let  $V_3(t) \in \mathbb{R}$  denotes the following non-negative function

$$V_3 \triangleq \frac{1}{2} y_a^2. \quad (69)$$

After taking the time derivative of (69), the following simplified expression can be obtained

$$\begin{aligned} \dot{V}_3 &= -k_{s1} \|J_s (I_n - J^+ J)\|^2 y_a^2 \\ &+ y_a \left[ J_s J^+ \Lambda^{-1} \begin{bmatrix} \dot{p}_d + K_1 e_p \\ -R_d^T \omega_d + K_2 e_v \end{bmatrix} - J_s r \right] \end{aligned} \quad (70)$$

where (44) was utilized. From (39), (41), (56), and the fact that  $p(t) \in \mathcal{L}_\infty$  from Theorem 1, Remark 2 can be used to show that  $\theta(t) \in \mathcal{L}_\infty$ ; hence, it is clear that  $J_s(\theta) \in \mathcal{L}_\infty$  for all sub-tasks. From Remark 1, it is clear that  $J(\theta)$  and  $J^+(\theta) \in \mathcal{L}_\infty$  and has full rank. Utilizing these properties we have

$$\|J_s (I_n - J^+ J)\|^2 > \bar{\delta} \quad (71)$$

where  $\bar{\delta} \in \mathbb{R}$  is a positive constant. From the above boundedness statements, and the boundedness assumptions placed on the desired trajectory, the following upper bound can be made

$$\left\| J_s J^+ \Lambda^{-1} \begin{bmatrix} \dot{p}_d + K_1 e_p \\ -R_d^T \omega_d + K_2 e_v \end{bmatrix} - J_s r \right\| \leq \delta_1 \quad (72)$$

where  $\delta_1 \in \mathbb{R}$  is a positive constant. After applying the bounds defined in (71) and (72), the expression in (70) can be written as follows

$$\dot{V}_3 \leq -k_{s1} \bar{\delta} y_a^2 + \delta_1 y_a. \quad (73)$$

The expression in (73) can be written as follows

$$\dot{V}_3 \leq -\left(k_{s1} \bar{\delta} - \frac{1}{\delta_2}\right) y_a^2 + \delta_1^2 \delta_2 \quad (74)$$

where the following inequality was utilized

$$|\delta_1 y_a| \leq \frac{1}{\delta_2} y_a^2 + \delta_1^2 \delta_2 \quad (75)$$

where  $\delta_2 \in \mathbb{R}$  is a positive constant. Provided  $k_{s1}$ ,  $\bar{\delta}$ , and  $\delta_2$  are selected according the following condition

$$\left(k_{s1} \bar{\delta} - \frac{1}{\delta_2}\right) > 0 \text{ then } k_{s1} > \frac{1}{\bar{\delta} \delta_2}, \quad (76)$$

the expression in (74) can be written as follows

$$\dot{V}_3 \leq -\gamma y_a^2 + \varepsilon \quad (77)$$

where  $\gamma, \varepsilon \in \mathbb{R}^+$  are bounding constants. After substituting (69) into (77), the following expression can be written

$$\dot{V}_3 \leq -2\gamma V_3 + \varepsilon. \quad (78)$$

After integrating each side of (78), the following solution can be written

$$V_3(t) \leq V_3(t_0) \exp(-2\gamma t) + \frac{\varepsilon}{2\gamma} (1 - \exp(-2\gamma t)). \quad (79)$$

From (79), it is clear that the following upper bound for  $y_a(t)$  can be written

$$|y_a(t)| \leq \sqrt{|y_a^2(t_0)| \exp(-2\gamma t) + \frac{\varepsilon}{\gamma}} \quad (80)$$

thus proving that  $y_a(t) \in \mathcal{L}_\infty$ . From (43), it is clear that  $h(\theta) \in \mathcal{L}_\infty$ . Utilizing the previous bounding statements with (44) it is clear that  $\dot{y}_a(t) \in \mathcal{L}_\infty$ . After taking the time derivative of (43), it is clear that  $\frac{\partial h(\theta)}{\partial \theta} \in \mathcal{L}_\infty$ .